Influence of post deposition annealing on structural and electrical properties of magnetron sputtered $Al/(Ta_2O_5)_{0.85}(TiO_2)_{0.15}/p\text{-}Si$ structure

M. CHANDRA SEKHAR[a*], N. NANDA KUMAR REDDY[a], S. VICTOR VEDANAYAKAM[a], M. RAJA REDDY[a], S. UTHANNA[b]

[a]*Department of Physics, Madanapalli Institute of technology and Science, Angallu, Madanapalle, Andhra Pradesh, India*

[b]*Department of Physics, Sri Venkateswara University, Tirupati, Andhra Pradesh, India*

Thin films of $[(Ta_2O_5)_{0.85}(TiO_2)_{0.15}]$ were deposited on p-Si (100) substrates by DC reactive magnetron sputtering technique subsequently, the as-deposited films were annealed at various temperatures in the range 873 -1173 K. The composition and core level binding energies of the films were analyzed by XPS. X-ray diffraction results revealed that the as-deposited and the films annealed at 873 K was amorphous, where as the films annealed at ≥ 973 K were transformed to polycrystalline. The as-deposited $(Ta_2O_5)_{0.85}(TiO_2)_{0.15}$ film (300 nm thick) showed a low leakage current density of 7.7×10^{-5} A/cm^2 at 1.5 V and it was decreased to 1.1×10^{-6} A/cm^2 at 1173 K. The current conduction mechanisms in the $(Ta_2O_5)_{0.85}(TiO_2)_{0.15}$ films, was compared and correlated with the Poole - Frenkel and Schottky emissions.

(Received February 06, 2014; accepted November 13, 2014)

Keywords: X-ray diffraction, X-ray photoelectron spectroscopy, Scanning electron microscopy (SEM), Tantalum oxide, Poole-Frenkel and Schottky emissions

1. Introduction

Tantalum oxide (Ta_2O_5) is considered as the potential high-*k* candidate as an active dielectric in storage capacitor of dynamic memories [1]. The doping of Ta_2O_5 with a small quantity of proper elements such as Ti, Hf, Al, N, C, Zr is a promising way for improving the dielectric properties compared to Ta_2O_5 and suppressing the negative effect of SiO_2-like layer [2, 3]. Adding of third element into the Ta_2O_5 can change the crystallization temperature. Since the crystal structure and grain size are affected by the dopant concentration, the doping changes actually the crystallization mechanism of the films and by this way, affects the dielectric and electrical properties of the films. It has been reported electrical properties of Ta_2O_5 can be increased through 8 % substitution of TiO_2 [4]. The dielectric properties of films with addition of TiO_2 to Ta_2O_5 were found to be enhanced compared to those of Ta_2O_5, and the mechanism of improvement was considered to be that oxygen vacancies are compensated by Ti^{4+} ions that are incorporated into Ta^{5+} sites in the films [5]. Due to several advantages such as good homogeneity, uniform deposition over large area substrates and good adhesion to the substrates, the $(Ta_2O_5)_{0.85}(TiO_2)_{0.15}$ thin films fabricated by DC reactive magnetron sputtering technique has been extensively used in thin film technology [6]. Annealing process is a method used to enhance the quality of the crystal structure and exploit structural defects in the material. During thermal annealing, the morphology and structural properties of the thin films were changed significantly [7-9]. Annealing process is employed especially when we want to obtain better electrical and optoelectronic characteristics. Annealing at suitable temperatures, not only improve the crystalline quality of films but also gain much better ohmic contacts [10,11]. In particular, the annealing ambient plays a very significant role on the fabrication of the high-quality $(Ta_2O_5)_{0.85}(TiO_2)_{0.15}$ films. It is argued that the crystallinity of the $(Ta_2O_5)_{0.85}(TiO_2)_{0.15}$ thin films improves with the post-deposition annealing temperature because of the decrement in the structural defects [12–15]. For semiconductor devices the structural properties are very important, therefore, it is essential to investigate how thermal annealing process affects on these properties [16,17]. The main electrical parameters, such as barrier height (Φ_b), ideality factor (n), series resistance (Rs), and the interface states (Nss) of the metal-semiconductor (MS) and metal-insulator-semiconductor (MIS) structures, are affected strongly by the existence of an insulator layer, since the insulator layer increases the values of Φ_b, n, and Rs, thereby leading to a decrease in the reverse leakage current and Nss [18,19]. In the present work, the effect of

post deposition annealing on structural and electrical properties of magnetron sputtered Al/$(Ta_2O_5)_{0.85}(TiO_2)_{0.15}$ /p-Si films has been presented.

2. Experimental

Thin films of $(Ta_2O_5)_{0.85}(TiO_2)_{0.15}$ were deposited on p-Si (100) substrates by employing DC reactive magnetron sputtering. Pure titanium – tantalum mosaic target of 100 mm diameter and 3 mm thick was used for deposition of $(Ta_2O_5)_{0.85}(TiO_2)_{0.15}$ films. The vacuum pumping system employed for sputtering was a combination of diffusion and rotary pumps. The films were deposited at an oxygen partial pressure of 6×10^{-2} Pa and at sputter pressure of 0.5 Pa. The as-deposited films were annealed in air for 1 hour at different temperatures in the range 873 - 1173 K. After deposition of the films, MOS (metal/oxide/semiconductor) capacitors were fabricated with the configuration of Al/$(Ta_2O_5)_{0.85}(TiO_2)_{0.15}$/p-Si by deposition of aluminium as top electrode with area of 9×10^{-4} cm^2. The sample configurations for metal-insulator-semiconductor for electrical measurements are shown in Fig. 1. The core level binding energies of the films were analysed with X-ray photoelectron spectroscopy (XPS), crystallographic structure with X-ray diffraction (XRD). The surface morphology of the films was analyzed by scanning electron microscopy (SEM). The thickness of the films was measured by α- step profilometer. The current-voltage characteristics of the films were studied by using Hewlett Peckard pA meter.

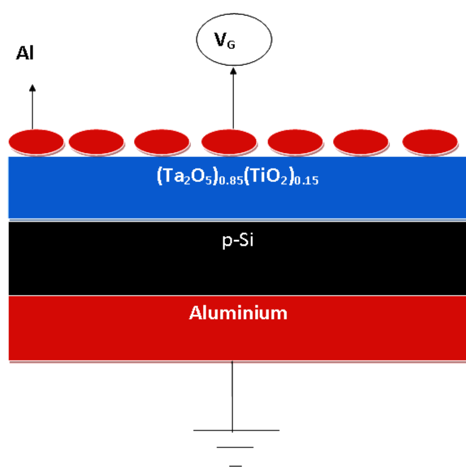

Fig. 1. Sample configuration for electrical measurement.

3. Results and discussion

Fig. 2 shows XPS survey scan spectra of the pure Ta_2O_5 and $(Ta_2O_5)_{0.85}(TiO_2)_{0.15}$ films formed on unheated silicon substrates. The pure Ta_2O_5 spectra contained the characteristic core level binding energies of Ta 4f, Ta 4d and O 1s, where as in $(Ta_2O_5)_{0.85}(TiO_2)_{0.15}$ films in addition to those present in pure Ta_2O_5, Ti 2P was also observed, it confirmed the presence of TiO_2. The narrow scan spectra of $(Ta_2O_5)_{0.85}(TiO_2)_{0.15}$ films showed the peaks at core level binding energies of about 26.2 and 28 eV related to Ta $4f_{7/2}$ and Ta $4f_{5/2}$ with spin orbit splitting of 1.8 eV, indicated the presence of tantalum in the oxidation state of Ta^{5+} [20]. The core level binding energy of $Ti2p_{3/2}$ and $Ti2p_{1/2}$ was 458.7 eV and 464.3 eV and the separation between the peaks is 5.6 eV indicated the presence of Ti^{4+} in oxidation state [21].The peak observed at about 530.2 eV was related to core level binding energy of O 1s. The ratios of tantalum to titanium (Ta/Ti) in the films were estimated from the XPS peak area using relative sensitivity factors. They had a value of nearly stoichiometric of $(Ta_2O_5)_{0.85}(TiO_2)_{0.15}$ films.

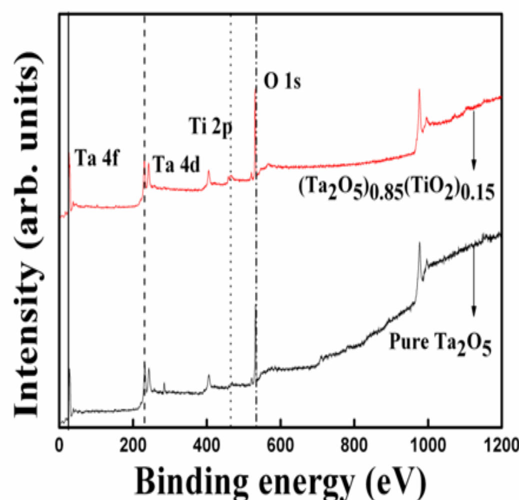

Fig. 2. Representative XPS survey scan spectra of pure Ta_2O_5 and $(Ta_2O_5)_{0.85}(TiO_2)_{0.15}$ films.

Fig. 3 shows the XRD patterns of the as deposited $(Ta_2O_5)_{0.85}(TiO_2)_{0.15}$ films and the films annealed in air at different temperatures. The as-deposited films were found to be X-ray amorphous. At the annealing temperatures ≥ 973 K, the diffraction peaks were observed at 2θ = 23.1, 28.4, 37.1, 47.2 and 55.9 ° related to the (101), (107), (116), (200) and (105) planes of β-Ta_2O_5 (JCPDS No.21-1199), whereas no diffraction peak was observed for TiO_2 due to its low content. Apparently, the peak intensity of (101) orientation had been prominent over other orientations [22]. As the annealing temperature was increased, the peaks in the XRD became sharper and the full width at half maximum (FWHM) decreased indicating the improvement in the crystallinity. The crystallite size was determined from the full width at half maximum of the diffraction peak at (101). The crystallite size of the films increased from 28 to 69 nm with increasing annealing temperature from 973 to 1173 K.

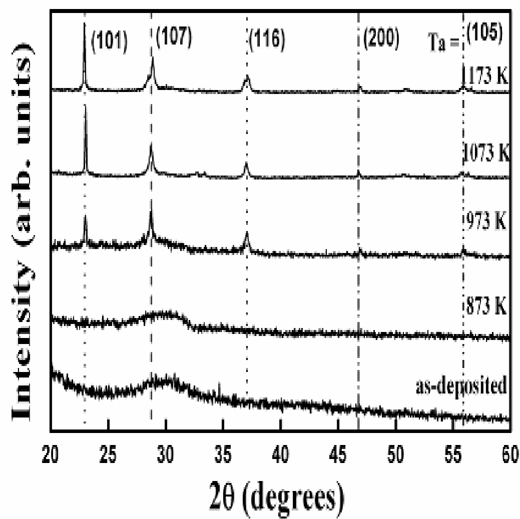

Fig. 3. X-ray diffraction profiles of $(Ta_2O_5)_{0.85}(TiO_2)_{0.15}$ films at different temperatures.

The scanning electron micrograph images of the $(Ta_2O_5)_{0.85}(TiO_2)_{0.15}$ films formed at different annealing temperatures are shown in Fig. 4. It is observed from the figure that the films deposited at 303 K showed very smooth morphology with out any fragmentation features indicated the fine grain structure in amorphous background. As the annealing temperature increased to 973 K, the crystallinity of the films was increased due to the coalescence of neighbouring crystallites driven by the thermal energy acquired from the heating treatment of the films. At annealing temperature 1173 K, the films were grown with spherical grain structures. The increase in crystallite size with increase of annealing temperature was attributed to the atomic, molecular or ionic species of $(Ta_2O_5)_{0.85}(TiO_2)_{0.15}$ impinged on the substrate surface acquire a large thermal energy and hence a large mobility. As a result, a large number of nuclei formed which coalescence at higher temperature to form a uniform film with good adhesion.

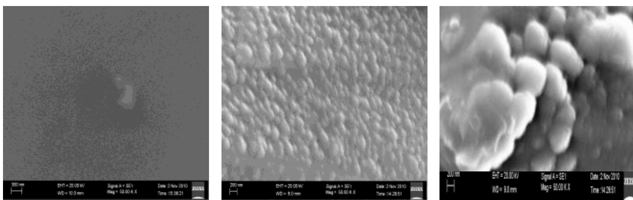

Fig. 4. SEM micrographs of $(Ta_2O_5)_{0.85}(TiO_2)_{0.15}$ films, (a) 303 K, (b) 873 K and (c) 1173 K.

Fig. 5 shows the leakage current density (J)-gate bias voltage (V_G) characteristics of the MOS [$Al/(Ta_2O_5)_{0.85}(TiO_2)_{0.15}/p\text{-}Si$] structured capacitors annealed at different annealing temperatures. The minimum leakage current density achieved at a gate bias voltage of 1.5 V was $7.7x10^{-5}$ A/cm^2 for as-deposited films. The leakage current density was decreased to $1.1x10^{-6}$ A/cm^2 by increasing the annealing temperature up to 1173 K. The I-V characteristics presented in the plot are exhibiting rectification or Schottky behaviour from 303 K to 1073 K. But, the I-V characteristic measured at 1173 K is seems to be non rectifying or ohmic. This may be due to the fact that, the electrical properties at the metal-semiconductor (MS) or metal-insulator-semiconductor (MIS) interface are governed by surface roughness [23] or interface state density [24]. According to Lucolano et al. [23] if surface roughness value is significant then the barrier height lowers, reverse leakage current increases and becomes non-rectifying or ohmic at 1173 K as evident from SEM analysis. However, Post-deposition annealing plays an important role in the improvement of crystallinity, reduction in oxygen ion vacancies, and increase in the packing density of the films which in turn reduce the leakage current density. The decrease in leakage current density with annealing temperature may be due to the increase in interfacial layer SiO_2 thickness and decrease in imperfections in the films. In the literature, it was observed that the leakage current density decreased, with the increase in annealing temperature with effect of interfacial layer growth [25,26]. The current density-voltage (J-V) dependence is linear at low fields indicating electron-hopping-conductivity i.e., the samples display nearly ohmic behavior. At intermediate fields, the current density was proportional to the square root of the applied electric field while at higher electric fields the current would be dominated by electron avalanche, because the current increased markedly with a small increase in the applied electric field. Figure 6 showed the Schottky conduction mechanism of the $Al/(Ta_2O_5)_{0.85}(TiO_2)_{0.15}/p\text{-}Si$ capacitors by plotting the graph between ln (J) versus $E^{1/2}$. From the Fig. 6 it is obvious that the logarithm of the current density is showing a linear relation with the applied electric field due to gate bias ($E^{1/2}$). This phenomenon is well established and is formulated to be Schottky emission at lower electric fields (< 1 MV/cm). The current conduction due to Schottky emission can be expressed as $J = A^*T^2 \exp[-q\Phi_B-\sqrt{qE/4\pi\varepsilon_r\varepsilon_o}/kT]$, Where $A^* = (4\pi qm^*k^2/h^3) = 120(m^*/m_o)$ A/cm^2k^2, A^* the effective Richardson constant, J the current density, T the absolute temperature, q the electronic charge, $q\Phi_B$ the Schottky barrier height, E the electric field, k the Boltzmann's constant, h the Plank's constant, ε_r the dynamic dielectric constant, ε_o the permittivity of free space and m* the effective electronic mass. The leakage current at higher fields may be due to the Poole-Frenkel (PF) conduction. PF emission is a major conduction process in insulators with a high impact of bulk traps and the conductivity is through the mediation of these traps.

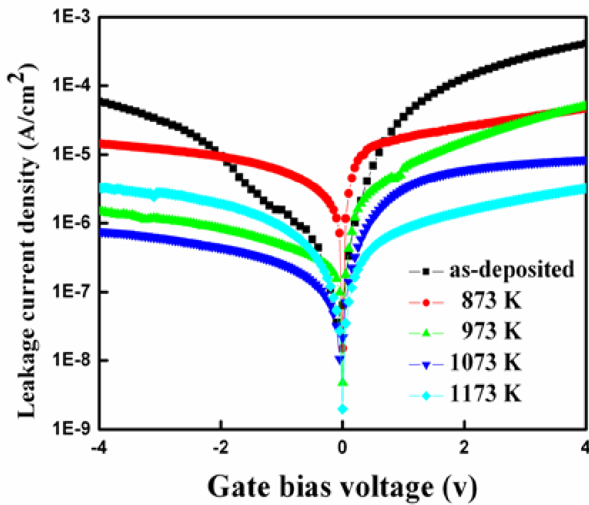

Fig. 5. Current density-Voltage (J-V) characteristics of Al/$(Ta_2O_5)_{0.85}(TiO_2)_{0.15}$/p-Si capacitors.

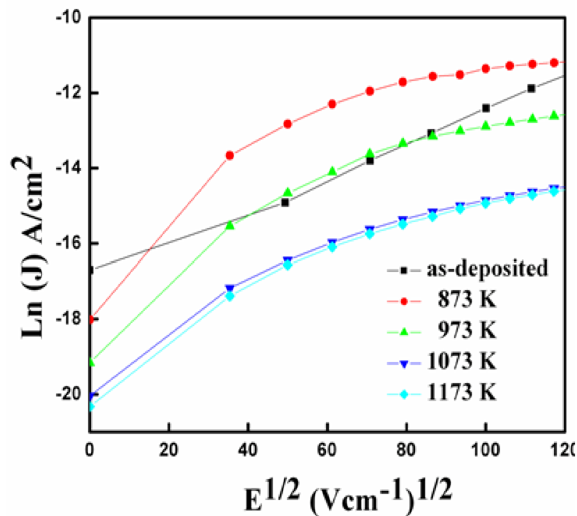

Fig. 6. Plots of $E^{1/2}$ versus ln (J) of Al/$(Ta_2O_5)_{0.85}(TiO_2)_{0.15}$/p-Si capacitors.

4. Conclusions

Thin films of $(Ta_2O_5)_{0.85}(TiO_2)_{0.15}$ were deposited on unheated p-Si substrates by means of DC reactive magnetron sputtering. The deposited films were annealed in air at temperatures in the range of 873-1173 K. The influence of post deposition annealing on core level binding energies, crystallographic structure and electrical properties were reported. The ratio of tantalum to titanium (Ta/Ti) in the films were estimated from the XPS peak area, and they had a value of nearly stoichiometric $(Ta_2O_5)_{0.85}(TiO_2)_{0.15}$ films. The as-deposited films were amorphous in nature, while at higher annealing temperatures it was transformed to polycrystalline. The surface morphology of the films was significantly varied with annealing temperature. The leakage current density of the films was high value at 303 K and it was decreased with the increase of annealing temperature at 1173 K. It can be attributed to the increase in interfacial layer SiO_2 thickness with the increase of annealing temperature. At higher electric fields the conduction mechanisms observed in the $(Ta_2O_5)_{0.85}(TiO_2)_{0.15}$ films was ascribed to the Poole-Frenkel emission, whereas, at low electric fields the dominance of Schottky emission. In conclusion, $(Ta_2O_5)_{0.85}(TiO_2)_{0.15}$ films formed at room temperature by DC magnetron sputtering were of amorphous in nature and the leakage current density of the $(Ta_2O_5)_{0.85}(TiO_2)_{0.15}$ films was high value of $7.7x10^{-5}$ A/cm^2. The films annealed at 1173 K were polycrystalline with low leakage current density of $1.1x10^{-6}$ A/cm^2. Hence, the post-deposition annealed $(Ta_2O_5)_{0.85}(TiO_2)_{0.15}$ films at 1173 K will be quite useful as a potential dielectric layer in MOS devices.

Acknowledgements

This work was carried out with the financial support of UGC, New Delhi, India through a sanctioned Major Research Project: F. No. 34-36/2008 (SR) dated: 30-12-2008. One of the authors, M. Chandra Sekhar thanks to UGC for sanctioned JRF under UGC-RFSMS scheme.

References

[1] E. Atanassova, A. Paskaleva, Microelectron. Reliab. **47**, 913 (2007).
[2] K. M. A. Salam, H. Fukuda, S. Nomura, J. Appl. Phys. **93**, 1169 (2003).
[3] D. H. Triyoso, R. I. Hedge, S. Zollner, J. Appl. Phys. **98**, 054104 (2005).
[4] R. F. Cava, W. F. Reck, Jr, J. J. Krajewski, Nature, **377**, 215 (1995).
[5] K. M. A. Salam, H. Fukuda, S. Nomura, J. Appl. Phys. **93**, 1169 (2003).
[6] M. Chandra Sekhar, S. Uthanna, R. Martins, S. V. Jagadeesh Chandra, E. Elangovan, IOP Conf. Series : Mater. Sci. Eng. **34,** 012009 (2012).
[7] F. Aziza, K. Sulaimana, M. R. Muhamyad, Kh. Karimov, World Academy of Science, Engineering and Technology **56**, 852 (2011).
[8] D. Gu, Q. Shenb, K. Liu, H. J. Xu, Thin Solid Films **257**, 88 (1995).
[9] S. Shihub, R. Gould, Physica Status Solidi A **139**, 129 (1993).
[10] C. F. Zhu, W. K. Fong, B. H. Leung, C. C. Cheng, C. Surya, IEEE Trans. Electron Dev. **48**, 1225 (2001).
[11] S. J. Cai, Y. S. Tang, R. Li, Y.Y. Wei, L. Wong, Y. L. Chen, K. L. Wang, M. Chen, Y. F. Zhao, R. D. Schrimpf, J. C. Keay, K. F. Galloway, IEEE Trans. Electron Dev. **47**, 304 (2000).
[12] H. Y. Yeom, N. Popovich, E. Chason, D. C. Paine,

Thin Solid Films **411**, 17 (2002).
[13] H. Morikawa, M. Fujita, Thin Solid Films **359**, 61 (2000).
[14] M. J. Alam, D. C. Cameron, Thin Solid Films **420–421**, 76 (2002).
[15] Y. S. Jung, Solid State Commun. **129**, 491 (2004).
[16] A. El-Bosaty, Egypt. J. Solids **29**, 1 (2006).
[17] M. Shah, Kh. S. Karimov, Semiconductor Science and Technology **25**, 75014 (2010). .
[18] Rhoderick E H andWilliams R H 1988 Metal-Semiconductor Contacts, 2nd edn. Oxford: Clarendon Press).
[19] Sze S M 1981 Physics of Semiconductor Devices, 2nd edn. (New York: John Wiley & Sons)
[20] R. Sanjines, H. Tang, H. Berger, F. Gozzo, G. Margaritondo, F. Levy, J. Appl. Phys. **75**, 2945 (1994).
[21] E. Atanassova, D. Spassov, Appl. Surf. Sci. **135**, 71 (1998).
[22] K. M. A. Salam, H. Konishi, M. Mizuno, H. Fukuda, S. Nomura, Appl. Surf. Sci. **190**, 88 (2002).
[23] F. Lucolano, F. Roccaforte, F. Giannazzo, V. Rainveri, J. Appl. Phys. **102**, 113701 (2007).
[24] F. Lucolano, F. Roccaforte, F. Giannazzo, V Rainveri, J. Appl. Phys. **104**, 093706 (2008).
[23] M. Nayak, T. Y. Tseng, Thin Solid Films **408**, 194 (2002).
[24] S. M. Chang, R. A. Doong, Thin Solid Films **489**, 17 (2005).

*Corresponding author: chandu.phys@gmail.com